A Novel Wedge Diffraction Modeling Using Method of Moments (MoM)

Gokhan Apaydin [1] and Levent Sevgi [2]

[1] Department of Electrical-Electronics Engineering
Zirve University, Gaziantep, 27260, Turkey
gokhan.apaydin@zirve.edu.tr

[2] Department of Electrical and Electronics Engineering
Okan University, Istanbul, 34959, Turkey
levent.sevgi@okan.edu.tr

Abstract ─ Scattering from edges and/or tips (i.e., diffraction) has long been modeled using different approaches. Initially, it was handled analytically using high frequency asymptotics (HFA). Parallel to the development in computer technology diffraction has begun to be modeled using numerical approaches also. Here, method of moments (MoM) is used to model the canonical wedge scattering problem and a novel, generally applicable procedure is introduced to extract diffracted fields and diffraction coefficients.

Index Terms ─ Diffraction, high frequency asymptotics, Method of Moments (MoM), wedge.

I. INTRODUCTION

The word *scattering* is used to represent all wave components produced from the interaction of electromagnetic (EM) waves with objects and include *incidence*, *reflection*, *refraction*, and *diffraction*. Mathematical (analytical) methods are used when frequency is high (i.e., when electromagnetic signal wavelength is quite low compared with the interacted object size) and these are geometric optics (GO), physical optics (PO), geometric theory of diffraction (GTD), uniform theory of diffraction (UTD), and physical theory of diffraction (PTD) [1-10]. GO is a ray-based approach which models incident, reflected, and refracted fields between source and receiver. PO, on the other hand, is an induced-surface-current based approach and models wave scattering caused by the induced-currents on the illuminated side of the object. Both GO and PO models are incapable of modeling edge and/or tip diffracted fields. These deficiencies were removed with the introduction of diffraction models GTD, UTD, and PTD. GTD takes into account diffraction everywhere except near critical angles and caustics. UTD can handle diffraction near critical angles but still suffers from caustics. Original PTD is general and can handle diffraction everywhere except near grazing incidence (this deficiency is then removed, see [2], Sec. 7.9). A very useful MatLab wedge diffraction package has been introduced for the illustration and visualization of all these HFA approaches [11].

Finite difference time domain (FDTD) method [12] is an effective approach in diffraction modeling [13-14]. A novel multi-step FDTD modeling has been introduced for the extraction of diffracted fields and diffraction coefficient [15]. A useful MatLab-based FDTD package was also introduced for the visualization of diffracted fields and for comparisons with several HFA models [16].

There have been several attempts in diffraction modeling using method of moments (MoM) in hybrid form [14-21]. The idea was to focus on and around the tip of the wedge and use MoM there; then combine the solution with one of the HFA approaches elsewhere. For example, MoM is combined with PO in [17] and then modified in [18] to overcome the failure of the hybrid approach in some cases. A similar hybridization example may be [19] where MoM was combined with the GTD. MoM solutions of wedge problems are well known and - in particular - adequate modeling by suitable basis-functions incorporating appropriate edge conditions well discussed in [20].

A novel two-step MoM [22] approach is introduced here for the extraction and visualization of diffracted fields on the canonical wedge scattering problem.

II. TWO DIMENSIONAL (2D) WEDGE SCATTERING AND DIFFRACTION MODELING

The non-penetrable wedge diffraction problem is canonical and plays a fundamental role in understanding and construction of HFA techniques as well as for the numerical tests. The exact solution to this scattering problem was first found by Sommerfeld [23] in the particular case of a half-plane. For the wedge with an arbitrary angle between its faces, the solution was

Submitted On: February 23, 2014
Accepted On: July 18, 2015

obtained by Macdonald and later on by Sommerfeld who developed the method of branched wave functions.

Figure 1 shows the 2D geometry of the semi-infinite wedge with PEC boundaries and exterior angle α. Wedge is located in a homogenous medium and illuminated by a cylindrical wave diverging from the line source $S(r_0,\varphi_0)$ and receiver point is given by $R(r,\varphi)$, where r,φ,z are the polar coordinates. The z-axis is aligned along the edge of the wedge. The angle φ is measured from the top face of the wedge. The time dependence $\exp(-i\omega t)$ is accepted in the paper.

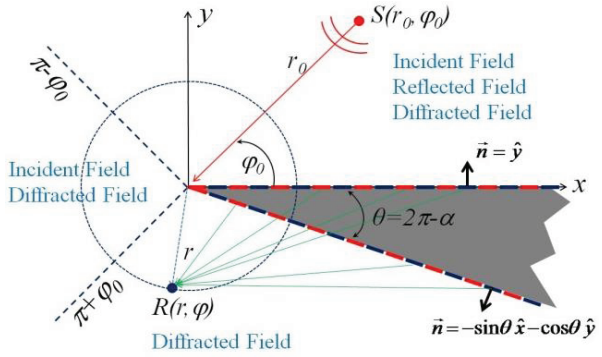

Fig. 1. 2D wedge geometry, line source and critical angles separating incident, reflected, diffracted fields.

The scenario in Fig. 1 ($0<\varphi_0<\alpha-\pi$) belongs to the single side illumination (SSI) where *the top face is illuminated*. In this case, the 2D scattering plane around the wedge may be divided into three regions in terms of critical wave phenomena occurring there. The region ($0<\varphi<\pi-\varphi_0$) includes all the field components - incident, reflected, and diffracted fields. The critical angle $\varphi=\pi-\varphi_0$ is called *Reflection Shadow Boundary (RSB)*. The region ($\pi-\varphi_0<\varphi<\pi+\varphi_0$) contains only incident and diffracted fields. The critical angle $\varphi=\pi+\varphi_0$ is the limiting boundary of the incident field and called *Incident Shadow Boundary (ISB)*. The third region ($\pi+\varphi_0<\varphi<\alpha$) is the shadow region where only diffracted fields exist.

The scenario with ($\alpha-\pi<\varphi_0<\pi$) belongs to the Double Side Illumination (DSI) where *both faces are always illuminated*. In this case, the 2D scattering plane around the wedge may also be divided into three regions. The regions ($0<\varphi<\pi-\varphi_0$) and ($2\alpha-\pi-\varphi_0<\varphi<\alpha$) contain all the field components. The region between these two (i.e., $\pi-\varphi_0<\varphi<2\alpha-\pi-\varphi_0$) contains no reflected fields and only incident and diffracted fields exist.

The field outside the wedge satisfies the Helmholtz's equation [1]:

$$\left(\frac{\partial^2}{\partial r^2}+\frac{1}{r}\frac{\partial}{\partial r}+\frac{1}{r^2}\frac{\partial^2}{\partial\varphi^2}+k^2\right)u=\frac{I_0}{r}\delta(r-r_0)\delta(\varphi-\varphi_0), \quad (1)$$

where k is the free-space wave number, I_0 is the line current amplitude, $\delta(\cdot)$ is the Dirac delta functions, the boundary conditions (BC) on $\varphi=0$ and $\varphi=\alpha$ are:

$$\text{(TM/SBC)}\, u_s=0 \text{ or (TE/HBC) } \partial u_h/\partial n=0, \quad (2)$$

and the Sommerfeld's radiation condition (SRC) at infinity is:

$$\lim_{r\to\infty}\sqrt{kr}\left(\frac{du}{dr}-iku\right)=0. \quad (3)$$

In the case of acoustic waves, either the field or its normal derivative is zero on the surface and these conditions refer to acoustically soft (SBC) and hard (HBC) wedges, respectively. In the case of EM waves, SBC and HBC correspond to the z-component of electric field intensity E_z (TM) and the z-component of magnetic field intensity H_z (TE), respectively. Non penetrable wedge corresponds to perfectly electrical/magnetic conductors for Dirichlet/Neumann (soft/hard or TM/TE) type BCs.

The total field solutions of the Helmholtz's equation with SBC and HBC for both SSI and DSI are [2]:

$$u_s^{tot}=\begin{cases}\dfrac{\pi I_0}{i\alpha}\displaystyle\sum_{l=1}^{\infty}J_{\nu_l}(kr)H_{\nu_l}^{(1)}(kr_0)\sin(\nu_l\varphi_0)\sin(\nu_l\varphi), & r\le r_0\\ \dfrac{\pi I_0}{i\alpha}\displaystyle\sum_{l=1}^{\infty}J_{\nu_l}(kr_0)H_{\nu_l}^{(1)}(kr)\sin(\nu_l\varphi_0)\sin(\nu_l\varphi), & r\ge r_0\end{cases}, \quad (4)$$

$$u_h^{tot}=\begin{cases}\dfrac{\pi I_0}{i\alpha}\displaystyle\sum_{l=0}^{\infty}\varepsilon_l J_{\nu_l}(kr)H_{\nu_l}^{(1)}(kr_0)\cos(\nu_l\varphi_0)\cos(\nu_l\varphi), & r\le r_0\\ \dfrac{\pi I_0}{i\alpha}\displaystyle\sum_{l=0}^{\infty}\varepsilon_l J_{\nu_l}(kr_0)H_{\nu_l}^{(1)}(kr)\cos(\nu_l\varphi_0)\cos(\nu_l\varphi), & r\ge r_0\end{cases}. \quad (5)$$

Here, $J_{\nu_l}(\cdot)$ and $H_{\nu_l}^{(1)}(\cdot)$ are Bessel and Hankel functions, respectively; $\nu_l=l\pi/\alpha$, and $\varepsilon_0=0.5$, $\varepsilon_1=\varepsilon_2=\varepsilon_3=\cdots=1$. The diffracted fields $u_{s,h}^{diff}$ can be calculated by subtracting the GO fields from (4) and (5) in different regions as:

$$u_{s,h}^{diff}=u_{s,h}^{tot}-\frac{I_0}{4i}u_{s,h}^{GO}, \quad (6)$$

where, for SSI ($0<\varphi_0<\alpha-\pi$):

$$u_{s,h}^{GO}=\begin{cases}H_0^{(1)}(kR_1)\pm H_0^{(1)}(kR_2) & 0<\varphi<\pi-\varphi_0\\ H_0^{(1)}(kR_1) & \pi-\varphi_0<\varphi<\pi+\varphi_0\\ 0 & \pi+\varphi_0<\varphi<\alpha\end{cases}, \quad (7)$$

and for DSI ($\alpha-\pi<\varphi_0<\pi$):

$$u_{s,h}^{GO}=\begin{cases}H_0^{(1)}(kR_1)\pm H_0^{(1)}(kR_2) & 0<\varphi<\pi-\varphi_0\\ H_0^{(1)}(kR_1) & \pi-\varphi_0<\varphi<2\alpha-\pi-\varphi_0\\ H_0^{(1)}(kR_1)\pm H_0^{(1)}(kR_3) & 2\alpha-\pi-\varphi_0<\varphi<\alpha\end{cases}, \quad (8)$$

where (-) and (+) are for SBC and HBC, respectively, and

$$R_1 = \sqrt{r^2 + r_0^2 - 2rr_0\cos(\varphi - \varphi_0)}\,, \quad (9a)$$

$$R_2 = \sqrt{r^2 + r_0^2 - 2rr_0\cos(\varphi + \varphi_0)}\,, \quad (9b)$$

$$R_3 = \sqrt{r^2 + r_0^2 - 2rr_0\cos(2\alpha - \varphi - \varphi_0)}\,. \quad (9c)$$

This model is based on the series summation in (4)-(5) and represents reference solution if computed accurately where the critical issue is the specification of the number of terms included which increases with frequency and/or distance.

III. MOM MODELING OF WEDGE SCATTERING

Method of moments (MoM) is a general procedure and frequency domain approach for solving linear equations. Many problems that cannot be solved *exactly* can be solved *approximately* by this method. The MoM owes its name to the process of taking moments by multiplying with appropriate *weighting* functions and integrating. It has been applied to a broad range of EM problems since the publication of the book by Harrington [22]. A comprehensive bibliography is too vast to be given here. A useful tutorial has just been published [24].

The MoM-based scattering model requires first analytical derivation of the 2D Green's function. Then, both surfaces of the wedge are discretized and replaced with a number of neighboring segments. The segment lengths are specified according to the wave frequency. As a rough criterion, the length of each segment should be equal to or less than one-tenth of the wavelength for discretization in almost all frequency and time domain models. At least ten segments per wavelength is a rough discretization; depending on the problem at hand as many as several dozen segments may be required. The number of segments on both surfaces are *N*, therefore the total number of segments is 2*N*. Note that, infinite distances, lengths, etc. can be truncated after several wavelengths (usually 10 to 100) with acceptable errors. Although it is an infinite wedge a rough truncation with ten to hundred wavelengths from the tip may be enough for the numerical simulations, depending on the polarization as well as other parameters.

Assuming that a line source illuminates the wedge, and currents induced on constant-length segments when illuminated by the source are constant, one can apply MoM technique and obtain the closed form matrix equation:

$$\bar{V} = \bar{\bar{Z}}\,\bar{I}\,, \quad (10)$$

where $\bar{I}$ contains the unknown segment currents, $\bar{V}$ denotes the incident field evaluated at the segment centers, and $\bar{\bar{Z}}$ is the $2N \times 2N$ impedance matrix [25].

The unknown segment currents are obtained by solving the system in (10). Finally, direct wave from the source to the receiver and scattered waves from all segments to the receiver are added and total wave at the observer is obtained.

Note that, each segment acts as a line source with omni-directional radiation pattern on *xz*-plane for the TM polarization. Therefore all segment currents are in parallel (and are perpendicular to the paper). Their mutual coupling (i.e., the impedance matrix) and scattered fields depend on only the distance. On the other hand, each segment acts as a short dipole for the TE polarization. Both their coupling and scattered fields are orientation (angle)-dependent.

IV. A NOVEL MOM PROCEDURE FOR THE EXTRACTION OF WEDGE DIFFRACTED FIELDS

Incident fields in MoM modeling are injected analytically using the Green's function solution of the problem at hand therefore the scattered fields accumulated from individual source-induced segment currents contain only reflected and diffracted fields. The critical angle $\varphi = \pi - \varphi_0$ (RSB) divides the whole scattering region into two; with and without reflected fields. As shown in Fig. 1, diffracted fields exist everywhere and reflected plus diffracted fields exist only in the region ($0 < \varphi < \pi - \varphi_0$). The MoM procedure of the wedge scattering is implemented as follows:

i. First, incident fields upon segments are calculated using the Green's function of the problem.
ii. The impedance matrix is formed.
iii. Then, 2*N* by 2*N* matrix system is solved and source-induced segment currents are obtained.
iv. Finally, scattered fields on the chosen observation points are calculated from the superposition of segment radiations using the Green's function.

The diffracted-only fields can be obtained using the MoM procedure if reflected fields in region ($0 < \varphi < \pi - \varphi_0$) are subtracted. The reflected fields in region ($0 < \varphi < \pi - \varphi_0$) can be extracted as follows:

- First, infinite-plane geometry shown in Fig. 2 is taken into account and standard 4-step MoM procedure explained above is applied. The MoM-computed scattered fields contain only reflected fields since there is no edge discontinuity.
- The scattered fields obtained with this geometry are subtracted from the scattered fields of the wedge geometry in region ($0 < \varphi < \pi - \varphi_0$) and reflected fields are all eliminated. The result yields diffracted-only fields.

Note that, reflected field regions are different for the DSI, therefore this procedure is repeated for $\varphi = \alpha$ plane and bottom-face-reflected fields are also extracted.

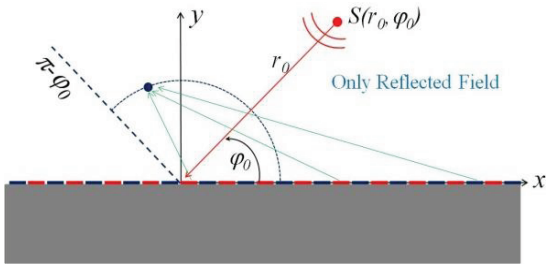

Fig. 2. Infinite-plane geometry and MoM modeling of scattered fields for the line source illumination. MoM-computed scattered fields contain only reflected fields.

Examples using this novel MoM procedure are shown in Figs. 3-7, where MoM-extracted diffracted fields for both polarizations are compared against the analytical reference solution as well as the uniform theory of diffraction (UTD) model. The total and diffracted fields are obtained.

A non-penetrable wedge with 60° interior angle is taken into account in Fig. 3. SBC (TM_z case) is assumed. Total and diffracted fields vs. angle around the tip of the wedge on a circle with 5λ-radius are plotted. The wedge is illuminated by a line source located 10λ-distance with φ_0=90°. Infinite wedge faces are truncated in 10λ and segment lengths are chosen λ/10. Total field vs. angle plots on the left show the three regions clearly. As observed, very good agreement is obtained with MoM modeling even with these rough discretization parameters.

A non-penetrable wedge with 90° interior angle is used in Fig. 4. All the parameters are kept the same as in Fig. 3 except the illumination angle (φ_0=60°). Again, total and diffracted fields vs. angle around the tip of the wedge are plotted and very good agreement is obtained among different models.

The next two examples belong to the other polarization (HBC/TE). In Fig. 5, a non-penetrable wedge with 60° interior angle is taken into account. Infinite wedge faces are truncated in 100λ in this case and segment lengths are chosen λ/20. Source and receiver distances from the tip of the wedge are kept the same. The illumination angle is 50°. Total and diffracted fields vs. angle around the tip of the wedge on a circle are plotted. MoM results are compared with exact series representation.

Figure 6 belongs to a non-penetrable wedge with 120° interior angle. HBC is used. The illumination angle is 30°. Total and diffracted fields vs. angle around the tip of the wedge are plotted using three different models.

The last example shows DSI case. Figure 7 belongs to a non-penetrable wedge with 90° interior angle for SBC case. The illumination angle is 120°. As observed, the agreement among the models is very good.

Note that, different discretizations are required for the TM (SBC) and TE (HBC) polarizations. Approximately, 10λ-long wedge sides are enough for the TM polarization and the results are in 200 by 200 matrix system. On the other hand, up to 100λ-long wedge sides (even more) may be required for the TE polarization where 2000 by 2000 matrix system is of interest. Nevertheless, both discrete systems can be solved within a minute with a regular student computer.

In addition, the frequency is fixed to 30 MHz in all the examples. It may be any value; there is no restriction as long as wavelength – distance relation is mentioned.

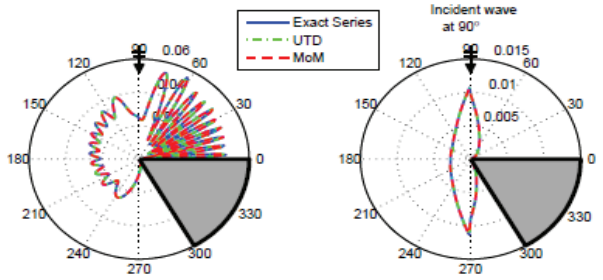

Fig. 3. Wedge scattering for TM/SBC: α=300°, r=50 m, r_0=100 m, φ_0=90°, and f=30 MHz; (left) total fields vs. angle, (right) diffracted fields vs. angle.

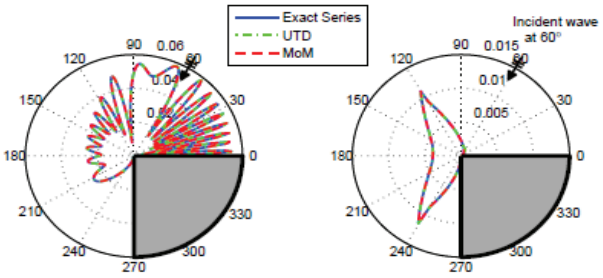

Fig. 4. Wedge scattering for TM/SBC: α=270°, r=50 m, r_0=100 m, φ_0=60°, and f=30 MHz; (left) total fields vs. angle, (right) diffracted fields vs. angle.

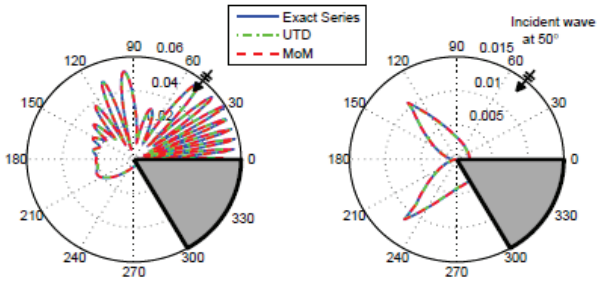

Fig. 5. Wedge scattering for TE/HBC: α=300°, r=50 m, r_0=100 m, φ_0=50°, and f=30 MHz; (left) total fields vs. angle, (right) diffracted fields vs. angle.

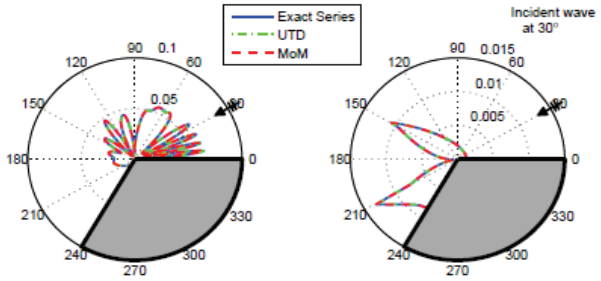

Fig. 6. Wedge scattering for TE/HBC: α=240°, r=50 m, r_0=100 m, φ_0=30°, and f=30 MHz; (left) total fields vs. angle, (right) diffracted fields vs. angle.

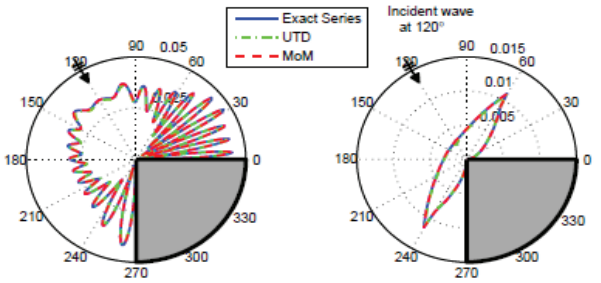

Fig. 7. Wedge scattering for TM/SBC: α=270°, r=50 m, r_0=100 m, φ_0=120°, and f=30 MHz; (left) total fields vs. angle, (right) diffracted fields vs. angle.

V. CONCLUSIONS

A novel Method of Moment (MoM) modeling is introduced for the calculation of diffracted fields in the frequency domain. Electromagnetic wave scattering from a non-penetrable wedge is taken into account and the edge-diffracted fields are extracted numerically. The results are validated against analytical reference solutions as well as the uniform theory of diffraction (UTD). This two-step MoM approach can be used to obtain the diffraction coefficients of scatterers with arbitrary shape and decomposition (e.g., loss-free and lossy dielectrics, metamaterials, etc.) [26]. Higher order diffraction effects can also be modeled, and, for example, double diffraction coefficients of multiple tips can be obtained.

Note that, the *diffraction coefficient* has a *physical meaning* only for high frequency fields and far away from the wedge when $kr_0 >> 1$, $kr >> 1$, and $r >> \lambda$ [15]. This term is a high frequency asymptotic (HFA) notion. One needs to reach at least r=10λ-20λ in order to obtain some reasonable values for diffraction coefficients. For an object of a size of several wavelengths, the size of MoM space reaches to hundreds by hundreds even in 2D which necessitates several thousand segments with a rough segment discretization of λ/10. This is within the range of applicability with a regular student computer with 2-4 GB RAM memory and a few GHz speed. Much larger memories are essential in 3D MoM modeling. Fortunately, there are alternatives and hybridization approaches to overcome these problems which are beyond the scope of this paper.

REFERENCES

[1] C. A. Balanis, *Advanced Engineering Electromagnetics*, Wiley, 2012.

[2] P. Ya. Ufimtsev, *Fundamentals of the Physical Theory of Diffraction*, Wiley, Hoboken, 2007.

[3] C. Balanis, L. Sevgi, and P. Ya Ufimtsev, "Fifty years of high frequency diffraction," *Int. J. RF Microw. Comput.-Aided Engrg.*, vol. 23, no. 4, pp. 394-402, July 2013.

[4] G. Pelosi, Y. Rahmat-Samii, and J. L. Volakis, "High frequency techniques in diffraction theory: 50 years of achievements in GTD, PTD, and related approaches," *IEEE Antennas Propag. Mag*., vol. 55, no. 3, pp. 16-17, June 2013.

[5] P. Ya. Ufimtsev, "The 50-year anniversary of the PTD: comments on the PTD's origin and development," *IEEE Antennas Propag. Mag*., vol. 55, no. 3, pp. 18-28, June 2013.

[6] Y. Rahmat-Samii, "GTD, UTD, UAT, STD: a historical revisit and personal observations," *IEEE Antennas Propag. Mag*., vol. 55, no. 3, pp. 29-40, June 2013.

[7] G. Pelosi and S. Selleri, "The wedge-type problem: the building brick in high-frequency scattering from complex objects," *IEEE Antennas Propag. Mag*., vol. 55, no. 3, pp. 41-58, June 2013.

[8] F. Hacivelioglu, L. Sevgi, and P. Ya. Ufimtsev, "Wedge diffracted waves excited by a line source: exact and asymptotic forms of fringe waves," *IEEE Trans. Antennas Propagat*., vol. AP-61, pp. 4705-4712, Sep. 2013.

[9] A. K. Gautesen, "Diffraction of plane waves by a wedge with impedance boundary conditions," *Wave Motion*, vol. 41, pp. 239-246, 2005.

[10] N. R. T. Biggs, "A new family of embedding formulae for diffraction by wedges and polygons," *Wave Motion*, vol. 43, pp. 517-528, 2006.

[11] F. Hacivelioglu, M. A. Uslu, and L. Sevgi, "A matlab-based virtual tool for the electromagnetic wave scattering from a perfectly reflecting wedge," *IEEE Antennas Propag. Mag*., vol. 53, no. 6, pp. 234-243, Dec. 2011.

[12] K. S. Yee, "Numerical solution of initial boundary value problems involving Maxwell's equations in isotropic media," *IEEE Trans. Antennas Propagat*., AP-14, pp. 302-307, 1966.

[13] V. Anantha and A. Taflove, "Efficient modeling of infinite scatterers using a generalized total-field/scattered field FDTD boundary partially embedded within PML," *IEEE Trans. Antennas Propagat*., AP-50, pp. 1337-1349, Oct. 2002.

[14] J.-H. Chang and A. Taflove, "Three-dimensional diffraction by infinite conducting and dielectric wedges using a generalized total-field/scattered-field FDTD formulation," *IEEE Trans. Antennas Propagat*., AP-53, pp. 1444-1454, Apr. 2005.

[15] G. Cakir, L. Sevgi, and P. Ya. Ufimtsev, "FDTD modeling of electromagnetic wave scattering from a wedge with perfectly reflecting boundaries: comparisons against analytical models and calibration," *IEEE Trans. Antennas Propagat*., AP-60, pp. 3336-3342, July 2012.

[16] M. A. Uslu and L. Sevgi, "Matlab-based virtual wedge scattering tool for the comparison of high frequency asymptotics and FDTD method," *Int. J. Appl. Comput. Electromagnet*., vol. 27, no. 9, pp. 697-705, Sep. 2012.

[17] H. J. Bilow, "Scattering by an infinite wedge with tensor impedance boundary conditions-a moment method/physical optics solution for the currents," *IEEE Trans. Antennas Propagat*., AP-39, pp. 767-773, June 1991.

[18] Z. Gong, B. Xiao, G. Zhu, and H. Ke, "Improvements to the hybrid MoM-PO technique for scattering of plane wave by an infinite wedge," *IEEE Trans. Antennas Propagat*., AP- 54, pp. 251-255, Jan. 2006.

[19] W. D. Burnside, C. L. Yu, and R. J. Marhefka, "A technique to combine the geometrical theory of diffraction and the moment method," *IEEE Trans. Antennas Propagat*., AP-23, pp. 551-558, July 1975.

[20] R. D. Graglia and G. Lombardi, "Singular higher-order divergence-conforming bases of additive kind and moments method applications to 3D sharp wedge structures," *IEEE Trans. Antennas Propagat*., AP-56, pp. 3768-3788, Dec. 2008.

[21] U. Jakobus and F. M. Landstorefer, "Improvement of the PO-MoM hybrid method by accounting for effects of perfectly conducting wedges," *IEEE Trans. Antennas Propagat.*, AP-43, pp. 1123-1129, Oct. 1995.

[22] R. F. Harrington, *Field Computation by Moment Method*, New York: IEEE Press, 1993.

[23] A. Sommerfeld, "Mathematische theorie der diffraction," *Mathematische Annalen*, vol. 16, pp. 317-374, 1896.

[24] E. Arvas and L. Sevgi, "A tutorial on the method of moments," *IEEE Antennas Propag. Mag*., vol. 54, no. 3, pp. 260-275, June 2012.

[25] G. Apaydin and L. Sevgi, "Method of moment (MoM) modeling for resonating structures: propagation inside a parallel plate waveguide," *Int. J. Appl. Comput. Electromagnet*., vol. 27, no. 10, pp. 842-849, Oct. 2012.

[26] M. A. Uslu, G. Apaydin, and L. Sevgi, "Double tip diffraction modeling: finite difference time domain vs. method of moments," *IEEE Trans. Antennas Propagat*., AP-62, pp. 6337-6343, Dec. 2014.

Gökhan Apaydin received the B.S., M.S., and Ph.D. degrees in Electrical & Electronics Engineering from Bogazici University, Istanbul, Turkey, in 2001, 2003, and 2007 respectively. He was a Teaching and Research Assistant with Bogazici University from 2001 to 2005; he was a Project and Research Engineer with University of Technology Zurich, Zurich, Switzerland from 2005 to 2010; and he was a Visiting Associate Professor with the Department of ECE, University of Illinois at Urbana-Champaign, IL, USA in 2015. Since 2010, he has been with Zirve University, Gaziantep, Turkey. He has been involved with complex electromagnetic problems and systems. His research study has focused on analytical and numerical methods in electromagnetics (especially on electromagnetic computation of wave propagation, diffraction modeling, and related areas).

Levent Sevgi received the Ph.D. degree from Istanbul Technical University (ITU), Turkey, and Polytechnic Institute of New York University, Brooklyn, in 1990. Prof. Leo Felsen was his advisor. He was with ITU (1991-1998); the Scientific and Technological Council of Turkey–Marmara Research Institute, Gebze/Kocaeli (1999-2000); Weber Research Institute/Polytechnic University in New York (1988-1990); the Scientific Research Group of Raytheon Systems, Canada (1998-1999); the Center for Defense Studies, ITUVSAM (1993-1998) and (2000-2002); the Department of ECE, UMASS Lowell, MA, USA (2012-2013) for his sabbatical term; and Dogus University (2001-2014). Since 2014, he has been with Okan University, Istanbul. He has been involved with complex electromagnetic problems and systems for nearly 30 years.